A DEM - FEM two scale approach of the behaviour of granular materials

Michał Nitka, Gabriela Bilbie, Gaël Combe, Cristian Dascalu and Jacques Desrues

Grenoble Universités, Laboratoire 3S-R, B.P. 53X, 38041 Grenoble, France

Abstract. We study the macroscopic behaviour of granular material, as a consequence of the interactions of individual grains at the micro scale. A two-scale approach of computational homogenization is considered. On the micro-level, we consider granular structures modelled using the Discrete Element Method (DEM). Grain interactions are modelled by normal and tangential contact laws with friction (Coulomb's criterion). On the macro-level, we use a Finite Element Formulation (FEM). The upscaling technique consists in using the response of the DEM model at each Gauss point of the FEM discretisation to derive numerically the constitutive response. In this process, a tangent operator is generated together with the stress increment corresponding to the strain increment in the Gauss point. In order to get more insight on the consistency of the resulting constitutive response, we compute the determinant of the acoustic tensor associated with the tangent operator. This quantity is known to be an indicator of a possible loss of uniqueness locally, at the macro scale, by strain localisation in shear band. Different numerical studies have been performed, as listed hereafter. We have considered different number of grains in the REV cell. Periodic boundary conditions have been compared with the ordinary wall conditions.

Keywords: Granular media, two-scale method, DEM, FEM, Acoustic tensor
PACS: 47.11.Fg, 04.60.Nc, 45.70, 46.25.Cc

INTRODUCTION

The objective of the study presented is to connect micro and macro computational methods in a unified two-scale approach. At the micro level, we consider granular model in 2D with round rigid bodies (grains) in the framework of molecular dynamic method (MD). At the macro level, we use a Finite Element Method (FEM) model. The link between the two scales is made through the constitutive response of the granular microstructure in a macroscopic Gauss point of the FEM model, which is obtained numerically. Indeed, by numerical homogenization of the results of the MD computations, we obtain the average stress over our REV as a response to the imposed FEM deformation history. In the same time, we derive numerically the tangent stiffness matrix at the Gauss point, and we are able to compute the acoustic tensor, which characterizes the possibility of instable behaviour. The stability zones depend on numerical parameters used in the computations. The influences of some of them are presented in what follows.

MECHANICAL MODELLING OF THE MICRO-SCALE: DEM

The system consist of a set of N polydisperse discs, with the random radii homogeneously distributed between R_{min} and $R_{max} = 2.5R_{min}$. This system is simulated using a discrete element method - molecular dynamic with a third-order predictor-corrector scheme [2]. All grains interact via a linear elastic law and Coulomb friction when they are in contact[1]. The normal contact force f_n is related to the normal apparent interpenetration δ of the contact as $f_n = k_n\delta$, where k_n is a normal stiffness coefficient ($\delta > 0$ if a contact is present, $\delta = 0$ if there is no contact). The tangential component f_t of the contact force is proportional to the tangential elastic relative displacement, with a tangential stiffness coefficient k_t . The Coulomb condition $|f_t| \leq \mu f_n$ requires an incremental evaluation of f_t in each time step, which leads to some amount of slip each time one of the equalities $f_t = \pm\mu f_n$ is imposed. A normal viscous component opposing the relative normal motion of any pair of grains in contact is also added to the elastic force f_n to obtain a critical damping of the dynamics. We consider two different boundary conditions: *Periodic Limit Condition* (PLC) and *rigid wall* (WLC), cf. Fig.1.

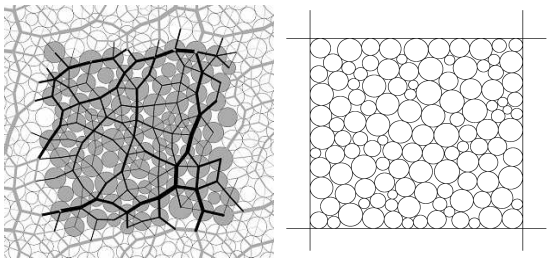

FIGURE 1. Shape of the PLC sample with normal contact forces (left) and cell of the sample with rigid walls (right)

MACRO LINK

Macroscopic constitutive law

For a given history of the deformation gradient, we need to calculate the global stress response. The macroscopic stress results from the average formula $\sigma_{ij} = \frac{1}{S}\sum_{c=1}^{N_c} f_i^c \cdot l_j^c;\ \ i,j \in \{x,y\}$, where S is the area of the sample, f_i^c and l_j^c are respectively the component i of the force acting in the contact c and the component j of the branch vector joining the mass centers of two grains in contact [3]. Next, we convert the Cauchy stress into the Piola-Kirhoff stress [4]. The Piola-Kirchoff stress is depended on the history of the *gradient of deformation* **F** [5], [6]

$$\overline{P}(t) = \Gamma^t\{\overline{F}(\tau), \tau \in [0,t]\} \tag{1}$$

For any history of $\overline{F}$, we assume that $\overline{P}$ admits at any time t a right derivative $\dot{\overline{P}}$ with respect to t:

$$\dot{\overline{P}} = lim_{\delta t \to 0} \frac{\overline{P}(t+\delta t) \ - \ \overline{P}(t)}{\delta t} \tag{2}$$

We assume also that, a history of $\overline{F}$ till time t being given, the right time derivative $\dot{\overline{P}}$ depends only on the right time derivative $\dot{\overline{F}}$ of $\overline{F}$:

$$\dot{\overline{P}} = \Theta(\dot{\overline{F}}) \tag{3}$$

where the function Θ is generally non-linear with respect to its argument $\dot{\overline{F}}$.
In the following, we limit the study to the case when the history of $\overline{F}$ is given by $\overline{F} = I + \alpha G^0$ with G^0 being a fixed tensor and α being the loading parameter which plays a role of t and runs monotonously from 0 to 1. In this case we get: $\dot{\overline{P}} = \Xi(\alpha)$ and by differentiating with respect to α, we get that $\dot{\overline{F}} = G^0$ along the path. According to the definition of the function Θ we can write the approximate formula [5], [6]:

$$\Theta(G^0) \approx \frac{\Xi(\alpha + \Delta\alpha) \ - \ \Xi(\alpha)}{\Delta\alpha} \tag{4}$$

Macroscopic loss of stability - Acoustic tensor

The loss of uniqueness for the rate of boundary value problems is analysed through Rice's approach [8]. Following this analysis we look for a rate gradient $\dot{\overline{F}}$ which is discontinuous along the boundary of a localization band. It is known that such a discontinuity can be written as [8]:

$$\dot{\overline{F^1_{kL}}} = \dot{\overline{F^0_{kL}}} + q_k N_l \tag{5}$$

where N is the normal ($||N|| = 1$) to the interface, $\dot{\overline{F^1}}$ is the rate gradient on the same side as N of the interface and $\dot{\overline{F^0}}$ on the other side. The stress vector has to be continuous through the interface, that reads:

$$\left(\dot{\overline{P^1_{iJ}}} \ - \ \dot{\overline{P^0_{iJ}}}\right) N_J \ = \ 0 \tag{6}$$

As $\dot{\overline{P^1_{iJ}}}$ and $\dot{\overline{P^0_{iJ}}}$ are linked to $\dot{\overline{F^1_{iJ}}}$ and $\dot{\overline{F^1_{iJ}}}$, by Eg. (3), the unknows **q** and **N** have to satisfy equation

$$\left(\Theta_{iJ}\left(\dot{\overline{F^0}} + q \otimes N\right) - \Theta_{iJ}\left(\dot{\overline{F^0}}\right)\right) N_J = 0 \tag{7}$$

where $\dot{\overline{F^0}}$ is given.
In the considered macroscopic quasistatic deformation process, the question of loss of ellipticity therefore comes down to determining the value α such as Eq. (7) has a non-trivial solution (q,N), $q \neq 0$.
In our case we restrict the search of a non-trivial solution to the case where the tensor $\overline{F^1}$ is closed to $\overline{F^0}$. This leads to a continuous bifurcation mode in the sense of Rice [8]. So, assuming that Θ is differentiable at $\dot{\overline{F^0}}$, eq. (7) yields after linearization:

$$B_{iJkL}\left(\dot{\overline{F^0}}\right) q_k N_L N_J = 0 \tag{8}$$

where $B_{iJkL}\left(\dot{\overline{F^0}}\right) = \frac{\partial \Theta_{iJ}}{\partial \dot{\overline{F}}_{kl}}|_{\dot{\overline{F}} = \dot{\overline{F^0}}}$ It is clear that a non-trivial solution exists only if the so-called *acoustic tensor* **Q** defined by $Q_{ik} = B_{iJkL} N_L N_J$ is singular, that is only if:

$$det\ Q = 0 \tag{9}$$

For this particular process considered here and given by $\overline{F} = I \ + \ \alpha G^0$, we have seen that $\dot{\overline{F}}$ is constant and equal to G^0, and the function $\Theta(G^0)$ can be approximated by Eq.(4).
As to the derivation of Θ, it can be numerically approximated by this finite difference:

$$B_{iJkL} = \frac{\Theta_{iJ}(G^0 + \varepsilon\Delta^{kL}) - \theta_{iJ}(G^0)}{\varepsilon} \tag{10}$$

where Δ^{kL} is a second-order tensor such as all its components are equal to 0 except kL which are equal to 1. Finally, in Fig. 2 we have calculated the stress at the point $\delta f \Delta\alpha$ (in the same linear direction as point n) and stresses in points with perturbations $\varepsilon\Delta^{kL}$. Than we have calculated the matrix tangent by [5], [6]:

$$B_{iJkL} = \frac{P_{iJ}(\alpha^{n+1} + \delta f \Delta\alpha + \varepsilon\Delta^{kL}) \ - \ P_{iJ}(\alpha^{n+1} + \delta f \Delta\alpha)}{\delta f \ \varepsilon\Delta^{kL}} \tag{11}$$

where $\delta f \Delta\alpha$ is a small variation step in the main direction, $\varepsilon\Delta^{kL}$ is a small perturbation in the direction kL.

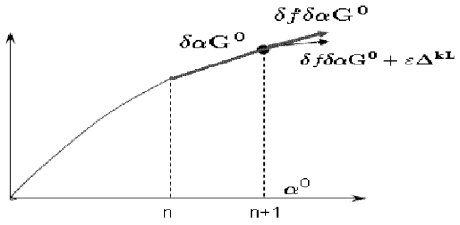

FIGURE 2. Schematic representation of the computation of the tangent matrix

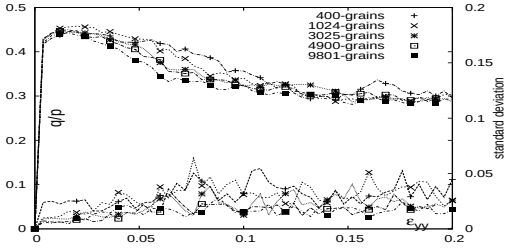

FIGURE 3. Mean stress and standard deviation for PLC samples

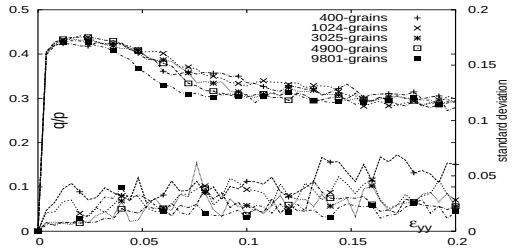

FIGURE 4. Mean stress and standard deviation for WLC samples

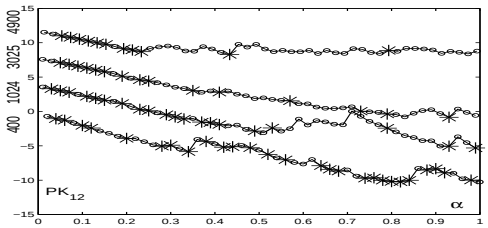

FIGURE 5. Influence of the size of sample on macroscopic stability (to be more clear diagrams are moved up on y-axis).

RESULTS

The normal stiffness of contact in the DEM is such that the stiffness parameter [9] $\kappa = k_n/\sigma_0 = 1000$, where σ_0 is an isotropic stress applied to the grain assemblies. The value of the tangential stiffness is equal to the normal stiffness $k_t = k_n$. Friction for the tangential contact law is taken as $\mu = 0.5$. All tests were done with similar *Inertial number* $I = \dot{\varepsilon}\sqrt{\frac{<m>}{\sigma_0}}$ [7], where $\dot{\varepsilon}$ is the strain rate, $< m >$ is the mean mass of grains. For all test I was set between $1.2 \cdot 10^{-3}$ to $2.1 \cdot 10^{-3}$ for iterations, and $6 \cdot 10^{-5}$ to $2.1 \cdot 10^{-3}$ for the small variation step $\delta f \Delta\alpha$.

We have considered different number of grains (from 400 to 9801) in samples and different boundary conditions.

The first test was made for a *biaxial* configuration with no volumetric changes, $\varepsilon_v = \varepsilon_{xx} + \varepsilon_{yy} = 0$. We have implemented a strain-controlled loading to get the overall stress response. The final strain is $\varepsilon = \begin{bmatrix} 0.2 & 0 \\ 0 & -0.2 \end{bmatrix}$ (negative values for compression). We have performed 10 tests for each size of sample and we have calculated mean values for stress and its standard deviations. Results of the stress-strain diagram for different size of the samples are presented for PLC on figure 3 and for WLC on figure 4. The y-axis is a q/p, where $q = (\sigma_{yy} - \sigma_{xx})/2$ and $p = (\sigma_{yy} + \sigma_{xx})/2$. We can observe that mean stress ratio q/p is increasing when the number of grains is decreasing, either for PLC and WLC. Nevertheless, this difference still small. On the other hand the standard deviation is decreasing with increase of sample size and over 3025 grains it is constant (figures 3 and 4).

Next, we performed tests for checking the stability in the macro level (biaxial test with and without volume changing, uniaxial and shearing) [8]. They were done for samples with 400, 1024, 3025 and 4900 grains.

The influence of the sample size for shearing test for Piola-Kirchhoff stress PK_{12} is presented on figure 5. Stars symbols represent instability points, that correspond to the $detQ < 0$, where Q is the acoustic tensor. This test was made for $\delta f = 0.1$ and perturbation $\varepsilon\Delta^{kL} = 2 \cdot 10^{-6}$. One can observe that if the size of sample the is increasing we obtain more important stability zones. We have also done tests to check the influence of the size of the small variation step $\delta f \Delta\alpha$ and the small perturbations $\varepsilon\Delta^{kL}$. Values for the small variation step δf were between 0.05 to 1 and for perturbations from $2 \cdot 10^{-6}$ to $2 \cdot 10^{-3}$. In this case we have obtained more stability zones for smaller values of small variation step $\delta f \Delta\alpha$ and for smaller values of perturbations value.

It is important to link macro-instability points with events representing their cause/origin at the micro level. To do this we are using the *fluctuation of the grain* $\vec{\delta}_i^{mn} = (\vec{r}_i^n - \vec{r}_i^m) - \Delta\varepsilon\vec{r}_i^m$, where $\vec{r}_i^m, \vec{r}_i^n$ are the positions of the grain i in steps m and n, respectively, and $\Delta\varepsilon$ is the increment of shear strain from step m to n. δ_{mn} is a displacement, that measures the shift of the grain with respect to its position as defined by the macroscopic

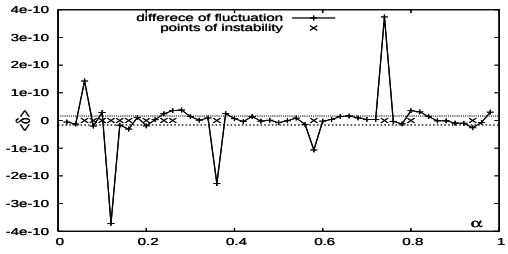

FIGURE 6. Fluctuation of grains for step α and perturbations (crosses correspond with the instability points)

strain Next we compute the mean value of fluctuation for all grains in the cell for one iteration ($\Delta\varepsilon$ is constant): $\langle\delta\rangle = \frac{1}{N}\sum_{i=1}^{N}\|\delta_i^{mn}\|^2$ where N is the number of grains.

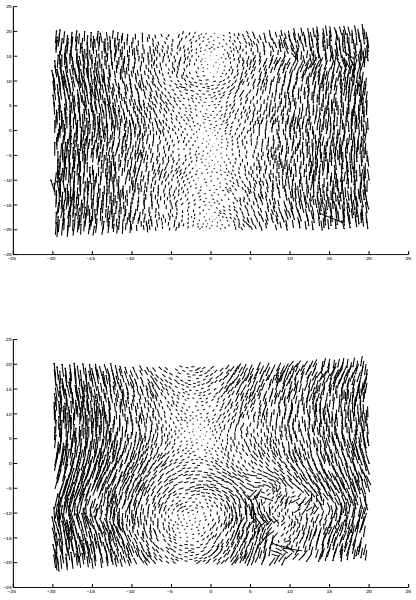

FIGURE 7. Maps of fluctuations for variation step for stability (top) and instability (bottom) points

In figure 6 we can observe differences between mean value of fluctuation for all four perturbations and fluctuation of the small variation step $\delta f\Delta\alpha = 0.1$ and instability zones in the sample with 3025 grains. One can observe that we have instability zones when the difference between fluctuations is big. If the difference is small normally we have stability.

In the figure 7 we have presented maps of fluctuations for shearing for small variation step $\delta f\Delta\alpha = 0.1$ for sample with 3025 grains. On the top we have fluctuations map for stability point and on the bottom for instability (for $\varepsilon_{12} = 0.102$ and $\varepsilon_{12} = 0.108$, respectively). The plotted idem is multiplied by 400 to make the diagram more clear.

One can see that at an instability point we get some 'relaxation' zone. We have observed that, in instability points, between small variation step and perturbations step we loose (or we get more) contacts between grains (or the normal forces are really small) . For stability we have almost no different of the number of contacts (one or two grains) while for instabilities this value is even 10 for all directions of perturbation.

CONCLUSIONS

We can observe that boundary condition has some influence on mean stress and standard deviation, but this influence is relatively small. For the mean stresses for PLC, the sample size does not play an important role, but for stability zones it has huge influence. It is very important for stability zone, to make the correct choice for the size of the sample (not too small). It is also very important to choose the correct small variation step δf and small perturbation $\varepsilon\Delta^{kL}$.
In the micro level we can observe a behaviour dependent on this coefficients, allowing us to identify the origin of instabilities in the macroscopic response. Some grains in instability regime loose their contact during small variation steps and perturbations. It is very important to reduce the number of those grains in every step (changing the numerical parameters). After resolving this problem, it is possible to connect the macro-micro codes and perform calculations for more complicated samples.

REFERENCES

1. P.A. Cundall and O.D.L. Strack, Géotechnique 29, No1, 47-65, 1979.
2. M. P. Allen and D. J. Tildesley, *Computer simulation of liqiuds*, Oxford Science Publications, 1994.
3. AEH Love, *A treatise on the mathematical theory of elasticity*, Cambridge University Press ,1927.
4. J. Bonnet and R. D . Wood, *Nonlinear continuum mechanics for finite element analysis*, Cambridge University, chap. 4, 1997.
5. G. Bilbie, C. Dascalu, R. Chambon, D. Caillerie, *Micro-fracture instabilties in granular solids*, in Bifurcations, Instabilities, Degradation in Geomechanics, Exadaktylos G. and Vardoulakis I. eds., pp. 231-242, 2007.
6. G. Bilbie, C. Dascalu, R. Chambon, D. Caillerie, Acta Geotechnica, vol. 3, pp 25-35, 2008.
7. J.-N. Roux,F. Chevoir, Bulletin des Laboratoires des Pontes et Chaussees, 245, 109-138, 2005.
8. J.R. Rice, *The localization of plastic deformation*, Koiter WT (ed) Theoretical and applied mechanics, 207-220, 1976.
9. G. Combe, J.-N. Roux, *Microscopic origins of quasi-static deformation in dense granular assemblies*, Powder and Grains 2001, Y. Kishoni, Ed., Balkema, pp 293-296, 2001.